Communications in Information and Systems
Volume 18, Number 4, 251–268, 2018

Series solution of a nonlocal dielectric test model for a solute ball with point charges in an ionic solvent

Hans W. Volkmer and Dexuan Xie†

This paper reports an analytical solution of a nonlocal dielectric test model for a solute ball with multiple point charges in an ionic solvent. The solution is derived in a single sum series of Legendre polynomials and modified spherical Bessel functions so that it can be calculated efficiently for a large set of charges or a large set of mesh points. It also contains the series solution of a two-region Kirkwood ball model as a special case. This series solution can be valuable in the study of nonlocal dielectric continuum models and in the validation tests on the numerical algorithms and software packages for solving nonlocal Poisson-Boltzmann equation models.

1. Introduction

Modeling and calculation of electrostatics for an ionic solvated protein is one fundamental task in biochemistry, biophysics, applied and computational mathematics, and bioengineering due to their essential roles in the prediction of biomolecular structures and properties. The Poisson-Boltzmann equation (PBE) is one widely used dielectric continuum model to do so [4, 5, 19] due to many PBE numerical algorithms developed by various advanced numerical techniques such as finite difference [3, 6, 13, 18], finite element [1, 19], and boundary element methods [10], along with its software packages [3, 14, 16, 25].

To reflect the polarization correlations of water molecules in the calculation of electrostatics, the nonlocal dielectric approach was proposed about forty years ago [8, 9, 17] (see [2] for a good review). Remarkably, it has been extended from a pure water solvent to an ionic solution in [22], and then led to a nonlocal modified Poisson-Boltzmann equation (NMPBE) for a protein in an ionic solvent in [20]. NMPBE is much more difficult to solve numerically

†Dexuan Xie is the corresponding author of this paper.

than PBE because of its position-dependent dielectric permittivity function over the whole space, which replaces PBE's piecewise constant permittivity function, and results in a derivative mixed convolution term. Even so, two efficient numerical algorithms and software packages were developed, respectively, in [20, 27], such that NMPBE becomes applicable in the calculation of electrostatic solvation and binding free energies.

However, how to validate or compare numerical algorithms and software packages for PBE and NMPBE remains an interesting research topic. In the early time, the so called Born ball models were constructed by Poisson dielectric models using a solute ball with one central point charge, and were used to validate and compare PBE's numerical solvers. As their extensions, we derived the exact solutions of three nonlocal Born ball test models in [23]. Moreover, we recently constructed two nonlocal Poisson dielectric test models using a solute ball containing multiple point charges, and then obtained their exact solution as single sum infinite series in terms of Legendre polynomials and modified spherical Bessel functions in [24]. These new test models have played important roles not only in the study of nonlocal dielectric models but also in the validation of NMPBE numerical solvers [20, 21, 24, 27].

Following what we did in [24], in this paper, we first construct a new nonlocal dielectric test model using a linear nonlocal PBE (LNPBE). Because of the new linear term caused by the ionic effects, new techniques are required to search for the exact solution of the new test model. One of them is reported in Lemma 1 to solve a system of coupled linear partial differential equations such that a solution of a fourth order differential equation is split as a sum of two second order equation solutions. In this way, we can express the exact solution in a series of Legendre polynomials and modified spherical Bessel functions.

As a local dielectric test model, the three-region Kirkwood ball model was proposed as early as 1930s, along with its exact solution in a double sum series due to using associated Legendre polynomials [7, 11, 15]. Here, a solute ball contains multiple charges, and is surrounded by a water region and an ionic solvent region. Such a series solution is rarely applied to the validation of PBE numerical solvers due to its complexity in calculation. By ignoring the water region, the three-region Kirkwood ball model is reduced to a two-region Kirkwood ball model, whose exact solution has been found in a single sum series (see [26] for example). In this paper, we show that the two-region Kirkwood ball model can be regarded as a special case of our nonlocal test model so that its series solution can be regained directly from the series solution of our nonlocal test model.

Finally, we programmed the series solutions of the nonlocal test model and the two-region Kirkwood ball model in Maple. We then did comparison tests with a solute ball containing one and three charges, respectively. Numerical test results demonstrate the differences between the local and nonlocal test models, and confirm that a nonlocal model can significantly reduce the solution region and improve the solution smoothness of the corresponding local model.

The remaining part of this paper is organized as follows. In Section 2, we present the nonlocal test model. In Section 3, we derive its series solution. Numerical results are reported in Section 4.

2. A nonlocal spherical dielectric test model

Let the whole space $\mathbb{R}^3$ be decomposed into a spherical solute region, $D_p = \{\mathbf{r} \mid |\mathbf{r}| < a\}$, a solvent region, $D_s = \{\mathbf{r} \mid |\mathbf{r}| > a\}$, and a spherical interface, $\Gamma = \{\mathbf{r} \mid |\mathbf{r}| = a\}$, such that

$$\mathbb{R}^3 = D_p \cup D_s \cup \Gamma. \tag{2.1}$$

Here, $a > 0$, D_s holds a symmetric 1:1 ionic solvent, and D_p contains n_p point charges with positions $\mathbf{r}_j$ and charge numbers z_j for $j = 1, 2, \ldots, n_p$. According to the NMPBE model [20], we define a nonlocal spherical test model as follows:

$$\begin{cases} -\epsilon_p \Delta u(\mathbf{r}) = \alpha \sum\limits_{j=1}^{n_p} z_j \delta_{\mathbf{r}_j}, & \mathbf{r} \in D_p, \\ -\epsilon_\infty \Delta u(\mathbf{r}) + \frac{\epsilon_s - \epsilon_\infty}{\lambda^2}[u(\mathbf{r}) - (u * Q_\lambda)(\mathbf{r})] + \kappa^2 u(\mathbf{r}) = 0, & \mathbf{r} \in D_s, \\ u(\mathbf{s}^-) = u(\mathbf{s}^+), & \mathbf{s} \in \Gamma, \\ \epsilon_p \frac{\partial u(\mathbf{s}^-)}{\partial \mathbf{n}(\mathbf{s})} = \epsilon_\infty \frac{\partial u(\mathbf{s}^+)}{\partial \mathbf{n}(\mathbf{s})} + (\epsilon_s - \epsilon_\infty) \frac{\partial (u * Q_\lambda)(\mathbf{s})}{\partial \mathbf{n}(\mathbf{s})}, & \mathbf{s} \in \Gamma, \\ u(\mathbf{r}) \to 0, \quad \text{as } |\mathbf{r}| \to \infty, \end{cases} \tag{2.2}$$

where u is a dimensionless electrostatic potential, D_p and D_s have been treated as two dielectric media with permittivity constants ϵ_p and ϵ_s, respectively, $\delta_{\mathbf{r}_j}$ is the Dirac delta distribution at $\mathbf{r}_j$, λ is a nonlocal parameter for characterizing the polarization correlations of water molecules, ϵ_∞ is another nonlocal parameter for indicating the dielectric constant for water in the case $\lambda \to \infty$, $\mathbf{n}(\mathbf{s})$ is the unit outward normal vector of D_p, α and κ are defined by

$$\alpha = \frac{10^{10} e_c^2}{\epsilon_0 k_B T}, \quad \kappa^2 = 2 \frac{10^{-17} N_A e_c^2}{\epsilon_0 k_B T} I_s, \tag{2.3}$$

and $u * Q_\lambda$ denotes the convolution of u with Q_λ, which is defined by

$$(u * Q_\lambda)(\mathbf{r}) = \int_{\mathbb{R}^3} Q_\lambda(\mathbf{r}-\mathbf{r}')u(\mathbf{r}')\mathrm{d}\mathbf{r}' \quad \text{with} \quad Q_\lambda(\mathbf{r}) = \frac{e^{-|\mathbf{r}|/\lambda}}{4\pi\lambda^2|\mathbf{r}|}.$$

Here, ϵ_0 is the permittivity of the vacuum, e_c is the electron charge, k_B is the Boltzmann constant, T is the absolute temperature, I_s is an ionic solvent strength, and N_A is the Avogadro constant.

Using the values of ϵ_0, e_c, T, k_B, and N_A given in Table 1 of [19], we can get

$$\alpha \approx 7042.9399, \qquad \kappa^2 \approx 8.4827\, I_s. \tag{2.4}$$

To avoid the calculation of the convolution term $u * Q_\lambda$, which is intricate, we treat the convolution $u * Q_\lambda$ as an unknown function, w, such that the test model (2.2) is reformulated as a partial differential equation interface system of two unknown functions, u and w, as follows:

$$-\epsilon_p \Delta u(\mathbf{r}) = \rho(\mathbf{r}), \qquad \mathbf{r} \in D_p, \tag{2.5a}$$

$$-\epsilon_\infty \Delta u(\mathbf{r}) + \frac{\epsilon_s - \epsilon_\infty}{\lambda^2}[u(\mathbf{r}) - w(\mathbf{r})] + \kappa^2 u(\mathbf{r}) = 0, \qquad \mathbf{r} \in D_s, \tag{2.5b}$$

$$-\lambda^2 \Delta w(\mathbf{r}) + w(\mathbf{r}) - u(\mathbf{r}) = 0, \qquad \mathbf{r} \in \mathbb{R}^3, \tag{2.5c}$$

$$u(\mathbf{s}^-) = u(\mathbf{s}^+), \quad \epsilon_p \frac{\partial u(\mathbf{s}^-)}{\partial \mathbf{n}(\mathbf{s})} = \epsilon_\infty \frac{\partial u(\mathbf{s}^+)}{\partial \mathbf{n}(\mathbf{s})} + (\epsilon_s - \epsilon_\infty)\frac{\partial w(\mathbf{s})}{\partial \mathbf{n}(\mathbf{s})}, \quad \mathbf{s} \in \Gamma, \tag{2.5d}$$

$$u(\mathbf{r}) \to 0, \quad w(\mathbf{r}) \to 0 \quad \text{as } |\mathbf{r}| \to \infty, \tag{2.5e}$$

where $\rho(\mathbf{r}) = \alpha \sum_{j=1}^{N} z_j \delta(\mathbf{r} - \mathbf{r}_j)$, and w satisfies the interface conditions

$$w(\mathbf{s}^-) = w(\mathbf{s}^+), \quad \frac{\partial w(\mathbf{s}^-)}{\partial \mathbf{n}(\mathbf{s})} = \frac{\partial w(\mathbf{s}^+)}{\partial \mathbf{n}(\mathbf{s})}, \quad \mathbf{s} \in \Gamma \tag{2.6}$$

due to the fact that w is twice continuously differentiable in $\mathbb{R}^3$.

3. Analytic solution of the test model

By the superposition principle, the solution (u, w) of the nonlocal spherical test model (2.5) can be expressed as

$$u(\mathbf{r}) = \alpha \sum_{j=1}^{n_p} z_j u_j(\mathbf{r}), \quad w(\mathbf{r}) = \alpha \sum_{j=1}^{n_p} z_j w_j(\mathbf{r}), \quad \mathbf{r} \in \mathbb{R}^3, \tag{3.1}$$

where α has been given in (2.3), and (u_j, w_j) denotes the solution of a special test model of (2.5) using $\rho(\mathbf{r}) = \delta(\mathbf{r} - \mathbf{r}_j)$. Thus, the remaining work for us to do is to derive the solution (u_j, w_j).

When $\mathbf{r}_j \neq \mathbf{0}$, the solution (u_j, w_j) is rotationally symmetric about the vector $\mathbf{r}_j$. That is, it depends only on two variables, r and ϕ_j, where $r = |\mathbf{r}|$, and ϕ_j denotes the angle between the two vectors $\mathbf{r}$ and $\mathbf{r}_j$ [24].

To look for the solution, we need the modified spherical Bessel functions $i_n(r)$ and $k_n(r)$ of the first kind and the second kind, respectively, and the Legendre polynomial P_n for $n = 0, 1, 2, \ldots$. As shown in [12, Section 10.47ff.], the derivatives $i_n'(r)$ and $k_n'(r)$ of $i_n(r)$ and $k_n(r)$ can be calculated by the formulas

$$i_n'(r) = \frac{n}{r} i_n(r) + i_{n+1}(r), \quad k_n'(r) = \frac{n}{r} k_n(r) - k_{n+1}(r). \tag{3.2}$$

We also cite the following two theorems from [12, Section 10.47ff.] for completeness.

Theorem 3.1. *If u is a rotationally symmetric solution to the Laplace equation $\Delta u = 0$ in D_p, then there are constants C_n such that*

$$u(\mathbf{r}) = \sum_{n=0}^{\infty} C_n r^n P_n(\cos\phi).$$

If u is a rotationally symmetric solution to the Laplace equation $\Delta u = 0$ in D_s with $u(\mathbf{r}) \to 0$ as $|\mathbf{r}| \to \infty$, then there are constants C_n such that

$$u(\mathbf{r}) = \sum_{n=0}^{\infty} C_n r^{-n-1} P_n(\cos\phi).$$

Theorem 3.2. *If u is a rotationally symmetric solution to $\Delta u - \kappa^2 u = 0$, $\kappa > 0$, in D_p, then there are constants C_n such that*

$$u(\mathbf{r}) = \sum_{n=0}^{\infty} C_n i_n(\kappa r) P_n(\cos\phi).$$

If u is a rotationally symmetric solution to $\Delta u - \kappa^2 u = 0$, $\kappa > 0$, in D_s with $u(\mathbf{r}) \to 0$ as $|\mathbf{r}| \to \infty$, then there are constants C_n such that

$$u(\mathbf{r}) = \sum_{n=0}^{\infty} C_n k_n(\kappa r) P_n(\cos\phi).$$

We now start to look for the solution with Lemma 1.

Lemma 1. *Let λ_1 and λ_2 be two distinct real numbers. If w satisfies the partial differential equation:*

$$(\Delta - \lambda_1)(\Delta - \lambda_2)w(\mathbf{r}) = 0, \quad \mathbf{r} \in D_s, \tag{3.3}$$

then w can be split as a sum of two functions, ζ_1 and ζ_2, in the form:

$$w(\mathbf{r}) = \zeta_1(\mathbf{r}) + \zeta_2(\mathbf{r}), \quad \mathbf{r} \in D_s, \tag{3.4}$$

where ζ_1 and ζ_2 satisfy the following two Laplace-like equations, respectively:

$$(\Delta - \lambda_1)\zeta_1(\mathbf{r}) = 0, \quad (\Delta - \lambda_2)\zeta_2(\mathbf{r}) = 0, \quad \mathbf{r} \in D_s. \tag{3.5}$$

Proof. We set

$$\zeta_1(\mathbf{r}) = \frac{1}{\lambda_1 - \lambda_2}(\Delta - \lambda_2)w(\mathbf{r}), \quad \zeta_2(\mathbf{r}) = -\frac{1}{\lambda_1 - \lambda_2}(\Delta - \lambda_1)w(\mathbf{r}).$$

Then (3.4) and (3.5) hold. □

We next present a general solution expression in Theorem 3.3.

Theorem 3.3. *If $\mathbf{r}_j \neq 0$, the general solution (u_j, w_j) of the spherical test model (2.5) using $\rho(\mathbf{r}) = \delta(\mathbf{r} - \mathbf{r}_j)$ has the series expressions:*

$$u_j(\mathbf{r}) = \begin{cases} \dfrac{1}{4\pi\epsilon_p}\dfrac{1}{|\mathbf{r} - \mathbf{r}_j|} + \displaystyle\sum_{n=0}^{\infty} A_{1n}|\mathbf{r}|^n P_n\left(\frac{\mathbf{r}_j \cdot \mathbf{r}}{|\mathbf{r}_j||\mathbf{r}|}\right), & \mathbf{r} \in D_p, \\ (1 - \lambda^2\eta_1^2)\displaystyle\sum_{n=0}^{\infty} A_{3n}k_n(\eta_1|\mathbf{r}|)P_n\left(\frac{\mathbf{r}_j \cdot \mathbf{r}}{|\mathbf{r}_j||\mathbf{r}|}\right) \\ \quad +(1 - \lambda^2\eta_2^2)\displaystyle\sum_{n=0}^{\infty} A_{4n}k_n(\eta_2|\mathbf{r}|)P_n\left(\frac{\mathbf{r}_j \cdot \mathbf{r}}{|\mathbf{r}_j||\mathbf{r}|}\right), & \mathbf{r} \in D_s, \end{cases} \tag{3.6}$$

and

$$w_j(\mathbf{r}) = \begin{cases} \dfrac{1-e^{-|\mathbf{r}-\mathbf{r}_j|/\lambda}}{4\pi\epsilon_p|\mathbf{r}-\mathbf{r}_j|} + \displaystyle\sum_{n=0}^{\infty} A_{1n}|\mathbf{r}|^n P_n\left(\frac{\mathbf{r}_j\cdot\mathbf{r}}{|\mathbf{r}_j||\mathbf{r}|}\right) \\ \quad + \displaystyle\sum_{n=0}^{\infty} A_{2n} i_n(\tfrac{|\mathbf{r}|}{\lambda}) P_n\left(\frac{\mathbf{r}_j\cdot\mathbf{r}}{|\mathbf{r}_j||\mathbf{r}|}\right), & \mathbf{r}\in D_p, \\ \displaystyle\sum_{n=0}^{\infty} A_{3n} k_n(\eta_1|\mathbf{r}|) P_n\left(\frac{\mathbf{r}_j\cdot\mathbf{r}}{|\mathbf{r}_j||\mathbf{r}|}\right) \\ \quad + \displaystyle\sum_{n=0}^{\infty} A_{4n} k_n(\eta_2|\mathbf{r}|) P_n\left(\frac{\mathbf{r}_j\cdot\mathbf{r}}{|\mathbf{r}_j||\mathbf{r}|}\right), & \mathbf{r}\in D_s, \end{cases} \tag{3.7}$$

where η_1 and η_2 are two positive constants defined by

$$\eta_1^2 = \frac{1}{2\epsilon_\infty\lambda^2}\left(\epsilon_s + \kappa^2\lambda^2 + \sqrt{(\epsilon_s+\kappa^2\lambda^2)^2 - 4\epsilon_\infty\lambda^2\kappa^2}\right), \tag{3.8}$$

$$\eta_2^2 = \frac{1}{2\epsilon_\infty\lambda^2}\left(\epsilon_s + \kappa^2\lambda^2 - \sqrt{(\epsilon_s+\kappa^2\lambda^2)^2 - 4\epsilon_\infty\lambda^2\kappa^2}\right), \tag{3.9}$$

and $\{A_{in}\}$ for $i = 1, 2, 3, 4$ are the coefficient sequences to be determined.

Proof. Let ϕ_j denote the angle between $\mathbf{r}$ and $\mathbf{r}_j$. Then,

$$\cos\phi_j = \frac{\mathbf{r}_j\cdot\mathbf{r}}{|\mathbf{r}_j||\mathbf{r}|}.$$

Using Theorem 3.1 and (2.5a), we obtain

$$u_j(\mathbf{r}) = \frac{1}{4\pi\epsilon_p}\frac{1}{|\mathbf{r}-\mathbf{r}_j|} + \sum_{n=0}^{\infty} A_{1n}|\mathbf{r}|^n P_n(\cos\phi_j), \quad \mathbf{r}\in D_p. \tag{3.10}$$

For $\mathbf{r}\in D_p$, a particular solution to (2.5c) is given by

$$\tilde{w}_j(\mathbf{r}) = \frac{1-e^{-|\mathbf{r}-\mathbf{r}_j|/\lambda}}{4\pi\epsilon_p|\mathbf{r}-\mathbf{r}_j|} + \sum_{n=0}^{\infty} A_{1n}|\mathbf{r}|^n P_n(\cos\phi_j).$$

Set $U(\mathbf{r}) = \frac{1}{4\pi\epsilon_p}\frac{1}{|\mathbf{r}-\mathbf{r}_j|}$. We then can get

$$(U * Q_\lambda)(\mathbf{r}) = \frac{1-e^{-|\mathbf{r}-\mathbf{r}_j|/\lambda}}{4\pi\epsilon_p|\mathbf{r}-\mathbf{r}_j|}.$$

Recall that $w_j = u_j * Q_\lambda$ and w_j satisfies the equation of (2.5c). Thus, the difference function $w_j - \tilde{w}_j$ gives a smooth solution of the equation

$$-\lambda^2 \Delta W + W = 0.$$

Therefore, by Theorem 3.2, w_j has a general expression of (3.7) in D_p.

We next look for the general solution expressions in the solvent region D_s.

Clearly, substituting (2.5c) into (2.5b) gives

$$\epsilon_\infty \lambda^2 \Delta^2 w(\mathbf{r}) - (\epsilon_s + \kappa^2 \lambda^2) \Delta w(\mathbf{r}) + \kappa^2 w(\mathbf{r}) = 0, \quad \mathbf{r} \in D_s.$$

We can factor the above quadratic equation in terms of the Laplace operator Δ in the form

$$(\Delta - \eta_1^2)(\Delta - \eta_2^2) w(\mathbf{r}) = 0, \quad \mathbf{r} \in D_s, \tag{3.11}$$

where η_1 and η_2 are given in (3.8) and (3.9). Since

$$(\epsilon_s + \kappa^2 \lambda^2)^2 - 4\epsilon_\infty \lambda^2 \kappa^2 = (\kappa^2 \lambda^2 - 2\epsilon_\infty + \epsilon_s)^2 + 4\epsilon_\infty (\epsilon_s - \epsilon_\infty),$$

which is positive due to the assumption that $0 < \epsilon_\infty < \epsilon_s$, we conclude that η_1 and η_2 are two distinct positive numbers. Thus, by Lemma 1, we get

$$w(\mathbf{r}) = \zeta_1(\mathbf{r}) + \zeta_2(\mathbf{r}), \qquad \mathbf{r} \in D_s, \tag{3.12}$$

where ζ_1 and ζ_2 satisfy the following partial differential equations:

$$\Delta \zeta_1 = \eta_1^2 \zeta_1, \quad \Delta \zeta_2 = \eta_2^2 \zeta_2 \quad \text{in } D_s. \tag{3.13}$$

Hence, the formula (2.5c) can be rewritten in the form

$$u = (1 - \lambda^2 \eta_1^2)\zeta_1 + (1 - \lambda^2 \eta_2^2)\zeta_2. \tag{3.14}$$

From Theorems 3.2 and the boundary condition (2.5e), we obtain the solutions of equations (3.13) in the expressions:

$$\zeta_1(\mathbf{r}) = \sum_{n=0}^{\infty} A_{3n} k_n(\eta_1 |\mathbf{r}|) P_n(\cos \phi_j),$$
$$\zeta_2(\mathbf{r}) = \sum_{n=0}^{\infty} A_{4n} k_n(\eta_2 |\mathbf{r}|) P_n(\cos \phi_j), \quad \mathbf{r} \in D_s.$$

Therefore, substituting the above expressions to (3.14) and (3.12) gives the general expressions (3.6) and (3.7) in D_s, respectively. This completes the proof of Theorem 3.3. □

Lemma 2. *Set* $\Lambda = \frac{\sqrt{\epsilon_\infty}}{\sqrt{\epsilon_s}}\lambda$. *Then the constants* η_1 *and* η_2 *defined by* (3.8) *and* (3.9), *respectively, satisfy*

$$0 < \eta_2 < \frac{1}{\lambda} < \frac{1}{\Lambda} < \eta_1. \tag{3.15}$$

Proof. We construct a quadratic polynomial, $h(z)$, in the expression

$$h(z) = \epsilon_\infty \lambda^2 z^2 - (\epsilon_s + \kappa^2\lambda^2)z + \kappa^2.$$

Clearly, η_1 and η_2 are the two roots of $h(z)$, and satisfy that

$$\eta_2^2 < \eta_1^2.$$

Since $\epsilon_s > \epsilon_\infty > 0$, we can find that

$$h(\lambda^{-2}) = \frac{\epsilon_\infty - \epsilon_s}{\lambda^2} < 0, \quad h(\Lambda^{-2}) = \frac{\epsilon_\infty - \epsilon_s}{\epsilon_\infty}\kappa^2 < 0,$$

from which it implies the inequalities of (3.15). □

We next obtain the solution in Theorem 3.4 through determining the coefficient sequences $\{A_{in}\}$ for $i = 1, 2, 3, 4$ of the general expressions (3.6) and (3.7) according to the interface conditions given in (2.5d) and (2.6).

Theorem 3.4. *The spherical test model* (2.5) *using* $\rho(\mathbf{r}) = \delta(\mathbf{r} - \mathbf{r}_j)$ *for* $\mathbf{r}_j \neq 0$ *has a unique solution,* (u_j, w_j), *in the series expressions of* (3.6) *and* (3.7), *where the series coefficients* A_{in} *for* $i = 1, 2, 3, 4$ *and* $n = 0, 1, 2, \ldots$ *are given in the expressions:*

$$A_{3n} = \frac{M_{2n}S_{1n} - L_{2n}S_{2n}}{L_{1n}M_{2n} - L_{2n}M_{1n}}, \qquad A_{4n} = \frac{L_{1n}S_{2n} - M_{1n}S_{1n}}{L_{1n}M_{2n} - L_{2n}M_{1n}}, \tag{3.16}$$

$$A_{1n} = \frac{1}{a^n}\left[A_{3n}(1-\lambda^2\eta_1^2)k_n(\eta_1 a) + A_{4n}(1-\lambda^2\eta_2^2)k_n(\eta_2 a) - \frac{r_j^n}{4\pi\epsilon_p a^{n+1}}\right], \tag{3.17}$$

$$A_{2n} = \frac{1}{i_n(\frac{a}{\lambda})}\left[A_{3n}\lambda^2\eta_1^2 k_n(\eta_1 a) + A_{4n}\lambda^2\eta_2^2 k_n(\eta_2 a) + \frac{2n+1}{2\pi^2\epsilon_p\lambda} i_n(\tfrac{r_j}{\lambda})k_n(\tfrac{a}{\lambda})\right]. \tag{3.18}$$

Here, $r_j = |\mathbf{r}_j|$, S_{1n} *and* S_{2n} *are defined by*

$$S_{1n} = \frac{(2n+1)r_j^n}{4\pi a^{n+1}}, \quad S_{2n} = \frac{2n+1}{4\pi\epsilon_p a^{n+1}}\left[i_n(\tfrac{a}{\lambda})r_j^n - i_n(\tfrac{r_j}{\lambda})a^n\right], \tag{3.19}$$

and L_{kn} and M_{kn} for $k = 1, 2$ are defined by

$$L_{kn} = \epsilon_p n(1-\lambda^2\eta_k^2)k_n(\eta_k a) - a\epsilon_s(1-\Lambda^2\eta_k^2)\eta_k k_n'(\eta_k a), \tag{3.20}$$

$$M_{kn} = a\lambda\eta_k^2 i_{n+1}(\tfrac{a}{\lambda})k_n(\eta_k a) + a\eta_k i_n(\tfrac{a}{\lambda})k_{n+1}(\eta_k a). \tag{3.21}$$

Proof. For every $n = 0, 1, 2, \ldots$, using the interface conditions (2.5d) and (2.6), we get a system of four linear equations for A_{in} for $i = 1, 2, 3, 4$ as follows:

$$\begin{aligned} &\frac{r_j^n}{4\pi\epsilon_p a^{n+1}} + A_{1n}a^n \\ &= A_{3n}(1-\lambda^2\eta_1^2)k_n(\eta_1 a) + A_{4n}(1-\lambda^2\eta_2^2)k_n(\eta_2 a), \end{aligned} \tag{3.22}$$

$$\begin{aligned} &-\frac{r_j^n(n+1)}{4\pi a^{n+2}} + A_{1n}\epsilon_p n a^{n-1} \\ &= A_{3n}\epsilon_s(1-\Lambda^2\eta_1^2)\eta_1 k_n'(\eta_1 a) + A_{4n}\epsilon_s(1-\Lambda^2\eta_2^2)\eta_2 k_n'(\eta_2 a), \end{aligned} \tag{3.23}$$

$$\begin{aligned} &\frac{r_j^n}{4\pi\epsilon_p a^{n+1}} - \frac{(2n+1)}{2\pi^2\epsilon_p\lambda} i_n\left(\tfrac{r_j}{\lambda}\right) k_n\left(\tfrac{a}{\lambda}\right) + A_{1n}a^n + A_{2n}i_n\left(\tfrac{a}{\lambda}\right) \\ &= A_{3n}k_n(\eta_1 a) + A_{4n}k_n(\eta_2 a), \end{aligned} \tag{3.24}$$

$$\begin{aligned} &-\frac{r_j^n(n+1)}{4\pi\epsilon_p a^{n+2}} - \frac{(2n+1)}{2\pi^2\epsilon_p\lambda^2} i_n\left(\tfrac{r_j}{\lambda}\right) k_n'\left(\tfrac{a}{\lambda}\right) + A_{1n}na^{n-1} + A_{2n}\tfrac{1}{\lambda}i_n'\left(\tfrac{a}{\lambda}\right) \\ &= A_{3n}\eta_1 k_n'(\eta_1 a) + A_{4n}\eta_2 k_n'(\eta_2 a). \end{aligned} \tag{3.25}$$

We multiply (3.22) by $\epsilon_p n$, (3.23) by $-a$, and add the equations to obtain

$$L_{1n}A_{3n} + L_{2n}A_{4n} = S_{1n}. \tag{3.26}$$

Then we multiply (3.22) by $-\frac{a}{\lambda}i_{n+1}(\frac{a}{\lambda})$, (3.24) by $\frac{a}{\lambda}i_n'(\frac{a}{\lambda})$, (3.25) by $-ai_n(\frac{a}{\lambda})$, and add the equations. From (3.2) we can get

$$\frac{a}{\lambda}i_n'\left(\frac{a}{\lambda}\right) = \frac{a}{\lambda}i_{n+1}\left(\frac{a}{\lambda}\right) + ni_n\left(\frac{a}{\lambda}\right).$$

We then use the above identity to obtain

$$M_{1n}A_{3n} + M_{2n}A_{4n} = S_{2n}, \tag{3.27}$$

where we have simplified the expressions for M_{kn} applying (3.2).

Let $\mathcal{D}$ denote the determinant of the coefficient matrix for the system of two linear equations (3.26) and (3.27) for unknowns A_{3n} and A_{4n}. It can be

found as

$$\mathcal{D} = L_{1n}M_{2n} - M_{1n}L_{2n}.$$

Using the fact that $i_n(r) > 0$, $k_n(r) > 0$, $k_n'(r) < 0$ for $r > 0$ and (3.15), we see that $L_{1n} < 0$, and the three numbers L_{2n}, M_{1n}, and M_{2n} are positive. Thus, the determinant $\mathcal{D}$ is negative (and nonzero). Hence, this system has a unique solution, and the solution can be found in the expressions of (3.16). Then (3.17) follows from (3.22), and (3.18) from (3.22) and (3.24). This completes the proof of Theorem 3.4. □

When the charge position $\mathbf{r}_j$ is at the origin, the solution (u_j, w_j) of the test model (2.5) with $\rho(\mathbf{r}) = \delta(\mathbf{r} - \mathbf{r}_j)$ becomes spherically symmetric. It can be obtained from (3.6) and (3.7) directly by only keeping the first term of each series (i.e., set all $A_{in} = 0$ except A_{i0}). In this case, $i_0(0) = 1$, the constants S_{10} and S_{20} of (3.19) are simplified as

$$S_{10} = \frac{1}{4\pi a}, \quad S_{20} = \frac{1}{4\pi\epsilon_p a}\left(i_0(\tfrac{a}{\lambda}) - 1\right),$$

and the constants L_{k0} and M_{k0} of (3.20) and (3.21) for $k = 1, 2$ become

$$\begin{aligned} L_{k0} &= -a\epsilon_s(1 - \Lambda^2\eta_k^2)\eta_k k_0'(\eta_k a), \\ M_{k0} &= a\lambda\eta_k^2 i_1(\tfrac{a}{\lambda})k_0(\eta_k a) + a\eta_k i_0(\tfrac{a}{\lambda})k_1(\eta_k a), \end{aligned}$$

where i_0, k_0, i_1, k_1, and k_0' are given as follows:

$$\begin{aligned} &i_0(r) = \frac{\sinh r}{r}, \quad k_0(r) = \frac{\pi}{2}\frac{e^{-r}}{r}, \quad i_1(r) = \frac{r\cosh r - \sinh r}{r^2}, \\ &k_1(r) = -k_0'(r) = \frac{\pi}{2}\frac{(r+1)}{r^2 e^r}. \end{aligned}$$

We present this special solution in Corollary 3.

Corollary 3. *The solution (u, w) of the test model (2.5) using $\rho(\mathbf{r}) = \delta(\mathbf{r})$ is given in the analytical expressions*

$$u(\mathbf{r}) = \begin{cases} \dfrac{1}{4\pi\epsilon_p}\dfrac{1}{|\mathbf{r}|} + A_{10}, & \mathbf{r} \in D_p, \\ (1 - \lambda^2\eta_1^2)A_{30}k_0(\eta_1|\mathbf{r}|) & \\ \quad +(1 - \lambda^2\eta_2^2)A_{40}k_0(\eta_2|\mathbf{r}|), & \mathbf{r} \in D_s, \end{cases} \tag{3.28}$$

and

$$w(\mathbf{r}) = \begin{cases} \dfrac{1-e^{-|\mathbf{r}|/\lambda}}{4\pi\epsilon_p|\mathbf{r}|} + A_{10} + A_{20} i_0(\frac{|\mathbf{r}|}{\lambda}), & \mathbf{r} \in D_p, \\ A_{30}k_0(\eta_1|\mathbf{r}|) + A_{40}k_0(\eta_2|\mathbf{r}|), & \mathbf{r} \in D_s, \end{cases} \tag{3.29}$$

where A_{30} and A_{40} are given in (3.16) *by setting $n = 0$, A_{20} is given by*

$$A_{20} = \frac{1}{i_0(\frac{a}{\lambda})}\left[A_{30}\lambda^2\eta_1^2 k_0(\eta_1 a) + A_{40}\lambda^2\eta_2^2 k_0(\eta_2 a) + \frac{1}{2\pi^2\epsilon_p\lambda}k_0(\tfrac{a}{\lambda})\right],$$

and A_{10} is given by

$$A_{10} = A_{30}(1-\lambda^2\eta_1^2)k_0(\eta_1 a) + A_{40}(1-\lambda^2\eta_2^2)k_0(\eta_2 a) - \frac{1}{4\pi\epsilon_p a}.$$

Remark. *Setting $\epsilon_\infty = \epsilon_s$, we can reduce the nonlocal spherical test model* (2.5) *to a two-region Kirkwood ball model as follows:*

$$\begin{cases} -\epsilon_p\Delta u(\mathbf{r}) = \alpha\sum_{j=1}^{N} z_j\delta(\mathbf{r}-\mathbf{r}_j), & \mathbf{r} \in D_p, \\ -\epsilon_s\Delta u(\mathbf{r}) + \kappa^2 u(\mathbf{r}) = 0, & \mathbf{r} \in D_s, \\ u(\mathbf{s}^-) = u(\mathbf{s}^+), \quad \epsilon_p\frac{\partial u(\mathbf{s}^-)}{\partial \mathbf{n}(\mathbf{s})} = \epsilon_s\frac{\partial u(\mathbf{s}^+)}{\partial \mathbf{n}(\mathbf{s})}, & \mathbf{s} \in \Gamma, \\ u(\mathbf{r}) \to 0 \qquad \textit{as } |\mathbf{r}| \to \infty. \end{cases} \tag{3.30}$$

Its series solution has been derived in [26]. It can also be derived directly from (3.6) *by setting $\epsilon_\infty = \epsilon_s$ because the local model* (3.30) *is a special case of the nonlocal model* (2.5)*. For completeness, we regain its series solution in our notation as follows:*

$$u(\mathbf{r}) = \alpha\sum_{j=1}^{n_p} z_j u_j(\mathbf{r}),$$

where u_j is given in the single sum series

$$u_j(\mathbf{r}) = \begin{cases} \dfrac{1}{4\pi\epsilon_p}\dfrac{1}{|\mathbf{r}-\mathbf{r}_j|} + \displaystyle\sum_{n=0}^{\infty} B_{1n} r^n P_n(\frac{\mathbf{r}_j\cdot\mathbf{r}}{|\mathbf{r}_j||\mathbf{r}|}), & \mathbf{r} \in D_p, \\ \displaystyle\sum_{n=0}^{\infty} B_{2n} k_n(\eta\mathbf{r}) P_n(\frac{\mathbf{r}_j\cdot\mathbf{r}}{|\mathbf{r}_j||\mathbf{r}|}), & \mathbf{r} \in D_s, \end{cases} \tag{3.31}$$

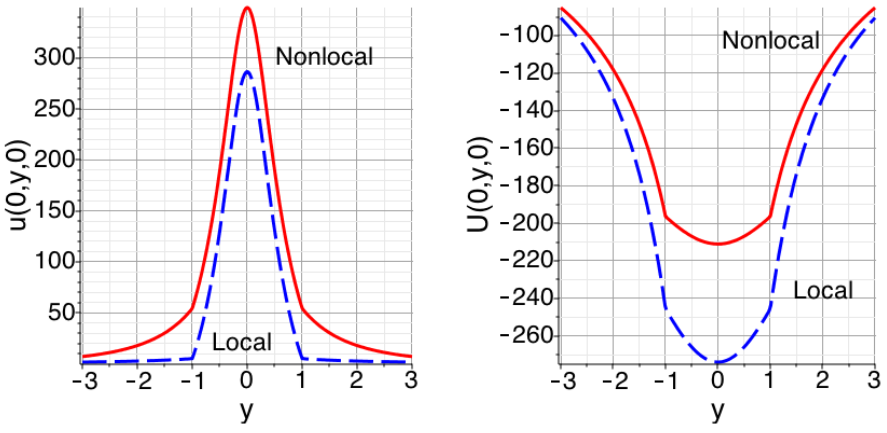

(a) Solution u (b) Reaction function U

Figure 1. A comparison of the nonlocal test model (2.5) with the two-region Kirkwood ball model (3.30) for the unit ball D_p with one unit positive charge at $(1/2, 0, 0)$.

with B_{1n} *and* B_{2n} *being defined by*

$$B_{1n} = \frac{|\mathbf{r}_j|^n}{4\pi a^{n+2} d_n} \left[\frac{\epsilon_s}{\epsilon_p} \eta a k_n'(\eta a) + (n+1) k_n(\eta a) \right], \tag{3.32}$$
$$B_{2n} = \frac{(2n+1)|\mathbf{r}_j|^n}{4\pi a^2 d_n}.$$

Here $d_n = \epsilon_p n a^{n-1} k_n(\eta a) - \epsilon_s a^n \eta k_n'(\eta a)$. *If* $r_j = 0$, $B_{1n} = B_{2n} = 0$ *for* $n \geq 1$, *and*

$$B_{10} = \frac{1}{4\pi\epsilon_s a^2 \eta k_1(\eta a)} \left[k_0(\eta a) - \frac{\epsilon_s}{\epsilon_p} \eta a k_1(\eta a) \right], \quad B_{20} = \frac{1}{4\pi\epsilon_s a^2 \eta k_1(\eta a)}.$$

4. Comparison tests

We programmed the series solution u of the nonlocal spherical test model (2.5), the series solution u of the two-region Kirkwood ball model (3.30), and the reaction function U in `Maple` worksheet (*https://www.maplesoft.com*). Here U is defined by

$$U(\mathbf{r}) = u(\mathbf{r}) - G(\mathbf{r}), \quad \mathbf{r} \in \mathbb{R}^3, \tag{4.1}$$

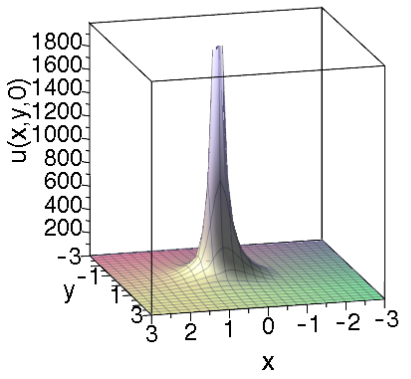

Figure 2. A surface of solution $u(x, y, 0)$ for $-3 \le x, y \le 3$ for the nonlocal model (2.5) using the unit ball D_p with one unit positive charge at $(1/2, 0, 0)$.

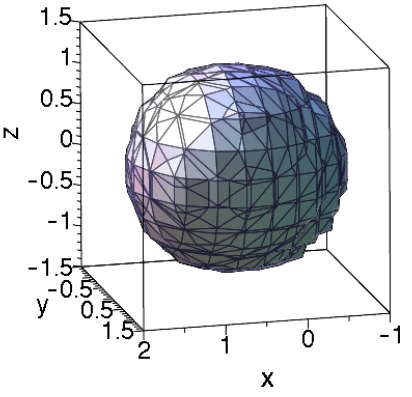

Figure 3. A contour surface defined by $u(x, y, z) = 50$ for the nonlocal model (2.5) using the unit ball D_p with one unit positive charge at $(1/2, 0, 0)$.

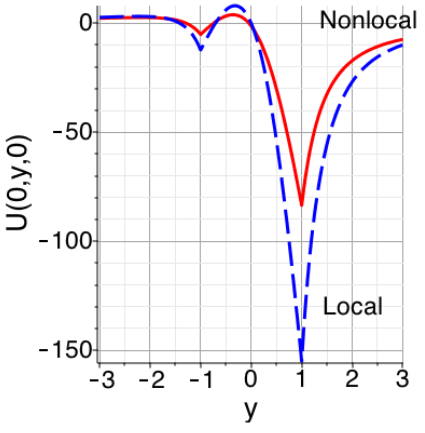

Figure 4. A comparison of the nonlocal test model (2.5) with the two-region Kirkwood ball model (3.30) for the unit ball D_p with three charges.

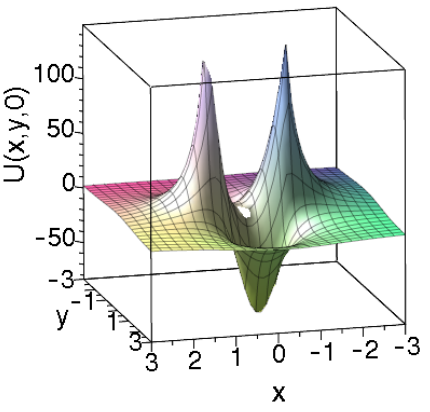

Figure 5. A surface of the reaction U as a function of x and y for $-3 \le x, y \le 3$ for the nonlocal test model (2.5) with three charges in the unit ball D_p.

where G is given in the expression

$$G(\mathbf{r}) = \frac{\alpha}{4\pi\epsilon_p} \sum_{j=1}^{n_p} \frac{z_j}{|\mathbf{r} - \mathbf{r}_j|}. \tag{4.2}$$

Since the solutions of the local and nonlocal models (2.5) and (3.30) share the same G, we may consider the reaction function U for a comparison of the local and nonlocal models. Note that G collects all the singularity points of u. Hence, U is continuous over the whole space and smooth within D_p and D_s, respectively. These properties are valuable for validating our series solutions and their numerical programs.

In the numerical tests, we set the physical parameters $\epsilon_p = 2$, $\epsilon_s = 80$, $\epsilon_\infty = 5$, $\lambda = 15$, and $I_s = 0.15$, which gave the model constants

$$\alpha \approx 7042.9399, \quad \kappa \approx 1.1280, \quad \eta_1 = 0.5675, \quad \eta_2 = 0.0592.$$

We then set the radius $a = 1$ for the solute region D_p, and approximated each series as a partial sum of N terms. We set $N = 20$ for all the tests, since it was found by numerical tests that a numerical value of u produced by using $N = 20$ had at most an error of 10^{-5} in comparison to a numerical value of u produced by using $N = 50$. We then used the formula (4.1) to calculate the reaction function U approximately.

We did tests for the unit ball region D_p containing one charge (i.e., $n_p = 1$) at position $\mathbf{r}_1 = (0.5, 0, 0)$ with charge number $z_1 = 1$. The numerical test results were reported in Figures 1 to 3.

Figure 1 compares the solution u and reaction function U of the nonlocal test model (2.5) with that of the two-region Kirkwood ball model (3.30), respectively, as a function of y for $-3 \le y \le 3$. From these test results it can be seen that the nonlocal test model (2.5) has significantly reduced the solution range and improved the solution smoothness of the local model (3.30).

To check the continuity of the nonlocal model solution u across the interface Γ, we found a value, 50, of u on Γ from Plot (a) of Figure 1. Here Γ is a unit sphere defined by the equation $x^2 + y^2 + z^2 = 1$ for $\mathbf{r} = (x, y, z)$. We then plotted a contour surface of the nonlocal model solution using the equation $u(x, y, z) = 50$ in Figure 3. Combining this figure with Figure 2, we can see that the series solution u of the nonlocal test model is continuous across the interface.

Furthermore, we calculated the local and nonlocal model solutions for the unit ball region D_p containing three charges (i.e., $n_p = 3$) at positions $\mathbf{r}_1 =$

$(-0.6, 0, -0.1)$, $\mathbf{r}_2 = (0, 0.2, 0.2)$, and $\mathbf{r}_3 = (0.6, 0.2, 0.1)$ with charge numbers $z_1 = -1$, $z_2 = 2$, and $z_3 = -1$, respectively. Figure 4 displays the differences between the local and nonlocal model solutions in terms of the reaction function U as a function of y for $-3 \le y \le 3$. These numerical results further confirm that the nonlocal test model has a much smaller solution region and a much smoother solution than the corresponding local model. Finally, Figure 5 further confirms the continuity of our series solution of the nonlocal test model (2.5).

References

[1] N. Baker, D. Sept, M. Holst, and J. A. McCammon, *The adaptive multilevel finite element solution of the Poisson-Boltzmann equation on massively parallel computers*, IBM Journal of Research and Development **45** (2001), 427–438.

[2] M. Basilevsky and G. Chuev, *Nonlocal solvation theories*, in: Continuum Solvation Models in Chemical Physics: From Theory to Applications, B. Mennucci and R. Cammi, eds., Wiley, 2008, pp. 94–109.

[3] D. Chen, Z. Chen, C. Chen, W. Geng, and G. Wei, *MIBPB: A software package for electrostatic analysis*, Journal of Computational Chemistry **32** (2011), 756–770.

[4] F. Fogolari, A. Brigo, and H. Molinari, *The Poisson-Boltzmann equation for biomolecular electrostatics: A tool for structural biology*, J. Mol. Recognit. **15** (2002), 377–392.

[5] B. Honig and A. Nicholls, *Classical electrostatics in biology and chemistry*, Science **268** (1995), 1144–1149.

[6] S. Jo, M. Vargyas, J. Vasko-Szedlar, B. Roux, and W. Im, *PBEQ-solver for online visualization of electrostatic potential of biomolecules*, Nucleic Acids Research **36** (2008), W270–W275.

[7] J. G. Kirkwood, *Theory of solutions of molecules containing widely separated charges with special application to zwitterions*, The Journal of Chemical Physics **2** (1934), 351.

[8] A. Kornyshev and G. Sutmann, *Nonlocal dielectric saturation in liquid water*, Phys. Rev. Lett. **79** (1997), 3435–3438.

[9] A. A. Kornyshev, A. I. Rubinshtein, and M. A. Vorotyntsev, *Model nonlocal electrostatics. I*, Journal of Physics C: Solid State Physics **11** (1978), 3307.

[10] B. Lu, X. Cheng, J. Huang, and J. A. McCammon, *AFMPB: An adaptive fast multipole Poisson-Boltzmann solver for calculating electrostatics in biomolecular systems*, Computer Physics Communications **181** (2010), 1150–1160.

[11] J. B. Matthew, *Electrostatic effects in proteins*, Annual Review of Biophysics and Biophysical Chemistry **14** (1985), 387–417.

[12] F. Olver, D. Lozier, R. Boisvert, and C. Clark, NIST Handbook of Mathematical Functions, Cambridge University Press, 2010.

[13] W. Rocchia, E. Alexov, and B. Honig, *Extending the applicability of the nonlinear Poisson-Boltzmann equation: Multiple dielectric constants and multivalent ions*, J. Phys. Chem. B **105** (2001), 6507–6514.

[14] S. Sarkar, S. Witham, J. Zhang, M. Zhenirovskyy, W. Rocchia, and E. Alexov, *Delphi web server: A comprehensive online suite for electrostatic calculations of biological macromolecules and their complexes*, Communications in Computational Physics **13** (2013), 269.

[15] C. Tanford and J. G. Kirkwood, *Theory of protein titration curves. i. general equations for impenetrable spheres*, Journal of the American Chemical Society **79** (1957), 5333–5339.

[16] S. Unni, Y. Huang, R. M. Hanson, M. Tobias, S. Krishnan, W. W. Li, J. E. Nielsen, and N. A. Baker, *Web servers and services for electrostatics calculations with APBS and PDB2PQR*, J. Comput. Chem. **32** (2011), 1488–1491.

[17] M. Vorotyntsev, *Model nonlocal electrostatics. II. Spherical interface*, Journal of Physics C: Solid State Physics **11** (1978), 3323.

[18] C. Wang, J. Wang, Q. Cai, Z. Li, H.-K. Zhao, and R. Luo, *Exploring accurate Poisson–Boltzmann methods for biomolecular simulations*, Computational and Theoretical Chemistry **1024** (2013), 34–44.

[19] D. Xie, *New solution decomposition and minimization schemes for Poisson-Boltzmann equation in calculation of biomolecular electrostatics*, J. Comput. Phys. **275** (2014), 294–309.

[20] D. Xie and Y. Jiang, *A nonlocal modified Poisson-Boltzmann equation and finite element solver for computing electrostatics of biomolecules*, Journal of Computational Physics **322** (2016), 1–20.

[21] D. Xie, Y. Jiang, P. Brune, and L. Scott, *A fast solver for a nonlocal dielectric continuum model*, SIAM J. Sci. Comput. **34** (2012), B107–B126.

[22] D. Xie, Y. Jiang, and L. Scott, *Efficient algorithms for a nonlocal dielectric model for protein in ionic solvent*, SIAM J. Sci. Comput. **38** (2013), B1267–1284.

[23] D. Xie and H. Volkmer, *A modified nonlocal continuum electrostatic model for protein in water and its analytical solutions for ionic Born models*, Commun. Comput. Phys. **13** (2013), 174–194.

[24] D. Xie, H. W. Volkmer, and J. Ying, *Analytical solutions of nonlocal Poisson dielectric models with multiple point charges inside a dielectric sphere*, Physical Review E **93** (2016), 043304.

[25] Y. Xie, J. Ying, and D. Xie, *SMPBS: Web server for computing biomolecular electrostatics using finite element solvers of size modified Poisson-Boltzmann equation*, Journal of Computational Chemistry **38** (2017), 541–552.

[26] Z. Xu, S. Deng, and W. Cai, *Image charge approximations of reaction fields in solvents with arbitrary ionic strength*, Journal of Computational Physics **228** (2009), 2092–2099.

[27] J. Ying and D. Xie, *An accelerated nonlocal Poisson-Boltzmann equation solver for electrostatics of biomolecule*, International Journal for Numerical Methods in Biomedical Engineering, online `https://doi.org/10.1002/cnm.3129`, 2018.

Hans W. Volkmer and Dexuan Xie:
Department of Mathematical Sciences
University of Wisconsin-Milwaukee
Milwaukee, WI 53201, USA
E-mail address: volkmer@uwm.edu
E-mail address: dxie@uwm.edu